Applied Catalysis B: Environmental 125 (2012) 85–94

Contents lists available at SciVerse ScienceDirect

Applied Catalysis B: Environmental

journal homepage: www.elsevier.com/locate/apcatb

Electrocatalytic oxidation of ethylene glycol (EG) on supported Pt and Au catalysts in alkaline media: Reaction pathway investigation in three-electrode cell and fuel cell reactors

Le Xin, Zhiyong Zhang, Ji Qi, David Chadderdon, Wenzhen Li*

Department of Chemical Engineering, Michigan Technological University, Houghton, MI 49931, USA

ARTICLE INFO

Article history:
Received 13 March 2012
Received in revised form 7 May 2012
Accepted 22 May 2012
Available online 30 May 2012

Keywords:
Electrocatalytic oxidation
Fuel cell
Alkaline electrolyte
Ethylene glycol
Reaction pathway

ABSTRACT

Carbon supported Pt and Au nanoparticles with small sizes (2.4 nm for Pt/C, and 3.5 nm for Au/C) and narrow size distributions were prepared though a modified solution-phase reduction method, and served as the working catalysts for an investigation of electrocatalytic oxidation of EG in alkaline media. Our three-electrode cell with an on-line sample collection system showed that with applied potential increasing, glycolic acid, oxalic acid and formic acid were sequentially produced from EG oxidation on Pt/C, while only glycolic acid and formic acid were detected on Au/C. Oxalic acid is a fairly stable product, and Pt/C is inactive to its further oxidation reaction. On Au/C, glycolic acid is the primary product, and no oxalic acid was found at specified test conditions. We clarified that formic acid was produced preferably from direct C—C bond cleavage of EG not glycolic acid on both Pt/C and Au/C catalysts. The single anion exchange membrane-direct EG fuel cell (AEM-DEGFC) with Pt/C and Au/C anode catalysts showed consistent results with the three-electrode cell tests. The AEM-DEGC with Pt/C anode catalyst demonstrated a peak power density of 71.0 mW cm^{-2}, which is much higher than that with the Au/C (only 7.3 mW cm^{-2}) at 50 °C. With the fuel cell operation voltage decreasing (anode overpotential increasing), deeper-oxidized products oxalic acid and formic acid were generated in the Pt/C anode AEM-DEGFC with higher selectivity. No formic acid was detected in the Pt anode AEM-DEGFC when glycolic acid was employed as fuel. On Au/C anode catalyst, very high selectivity to glycolic acid (>98%) was achieved. The AEM-DEGFC results confirmed the EG electro-oxidation pathways proposed by using an on-line sample collection system.

1. Introduction

Efficient catalytic transformation of chemical energy stored in small organic molecules directly into electrical energy for low temperature fuel cells has been a long-time research challenge [1–4]. Compared to methanol fuel, ethylene glycol (EG) has advantages of high volumetric energy density (5.9 kWh l^{-1} vs. 4.8 kWh l^{-1}), high boiling point (197 °C vs. 65 °C) and low toxicity, which makes it an attractive fuel for direct alcohol fuel cells (DAFCs) [4–6]. Additionally, recent studies found that EG can be directly produced from catalytic conversion of biomass-related cellulose with high yields [7,8]. This provides new opportunities for sustainable widespread applications of direct EG fuel cells (DEGFCs). However, the slow kinetics of electro-oxidation of small alcohols remains a long-standing scientific issue to developing efficient DAFCs [1–4]. Platinum (Pt) and gold (Au) have been investigated as catalysts for the electro-oxidation of EG for decades [9–15], and Pt exhibits higher electrocatalytic activity than Au. Furthermore, it has been found that in acid electrolyte, CO or CO-like intermediates may strongly adsorb on the active sites of Pt, resulting in catalyst poisoning; while Au is nearly inactive to EG electro-oxidation in acid media due to its weak adsorption capability. However, when high pH electrolyte is used, the high concentration of OH^- in the electrolyte and adsorbed hydroxyl on the Pt or Au surface are able to greatly facilitate the de-protonation of alcohols, and thus significantly lower the energy barrier of alcohol oxidation reactions [16,17]. Therefore, the alkaline media can improve the kinetics of EG electro-oxidation on both Pt and Au, and even make Au a possible anode catalyst for DEGFCs.

The electro-oxidation of EG is a complex process, involving various successive and parallel reaction pathways. To design efficient anode electrocatalysts for DEGFCs, it is of primary importance to understand the mechanisms of EG electro-oxidation on metal catalysts. A variety of analysis techniques, such as Fourier transform infrared (FTIR) spectroscopy [18], high performance liquid chromatography (HPLC) [14,19], and differential electrochemical mass spectrometry (DEMS) [20], etc. have been developed to analyze the reaction intermediates on catalyst surfaces and/or in

* Corresponding author. Tel.: +1 906 487 2298; fax: +1 906 487 3213.
E-mail address: wzli@mtu.edu (W. Li).

0926-3373/$ – see front matter © 2012 Elsevier B.V. All rights reserved.
http://dx.doi.org/10.1016/j.apcatb.2012.05.024

liquid electrolyte, thus to investigate the reaction pathways of EG electro-oxidation. With mass-spectroscopic investigation, reaction intermediates/products such as glycolaldehyde, glycolic acid, glyoxal, glyoxylic acid, oxalic acid, formic acid and CO were examined on a polycrystalline Pt electrode during the electro-oxidation of EG in alkaline electrolyte [12], while Christensen and co-workers used in situ FTIR spectroscopy to study the electro-oxidation of EG in alkaline media and found that glycolate, oxalate and carbonate were the main products on Pt electrode [11]. Analyses of the alkaline electrolyte solution after electro-oxidation of EG on Au electrode were also performed by combining HPLC and FTIR analyses. It was reported that at potentials less than 1.13 V vs. RHE, glycolate was the only product, whereas at potentials greater than 1.13 V, glycolate could be further oxidized to glyoxylate, oxalate and formate [9,10]. In addition, Weaver and co-workers proposed the C—C bond cleavage on Pt involved the short-lived surface intermediates, whereas on Au, it occurred involving long-lived solution-phase intermediates [18]. Based on HPLC analysis results, two parallel pathways were proposed regarding the EG electro-oxidation on Pt in alkaline media: a non-poisoning pathway which yielded oxalate without C—C bond scission, and a poisoning pathway which produced adsorbed CO species via the rupture of C—C bond of C_2 intermediates [14]. However, the pathways of EG electro-oxidation on Pt and Au in alkaline media are still unclear, in particular, the detailed pathway of C—C bond cleavage process. Recently, Koper's group developed an elegant on-line collection off-line HPLC analysis system. Combined with electrochemical voltammetry, they investigated the products of electro-oxidation of glycerol and some primary alcohols in situ generated close to the electrode surfaces in liquid electrolyte under accurately controlled potentials, and gained new insights into the oxidation pathways [21,22]. Currently, there is a clear need to examine the acquired reaction pathways in real fuel cell reactors, so as to help the development of more efficient anode catalysts for DEGFCs.

Recently we designed a similar on-line sample collection system, and linked it to a conventional three-electrode cell setup. Through a combined study of staircase linear scan voltammetry and cyclic voltammetry (CV) on supported Pt or Au nanoparticle catalysts (Pt/C and Au/C) in alkaline solution of EG, glycolic acid, and oxalic acid, we obtained the detailed reaction sequence of EG electro-oxidation on Pt/C and Au/C catalysts in high pH media. We further examined the catalytic functions (reactivity and selectivity) of Pt/C and Au/C anode catalysts in 'real' AEM-DEGFC reactors. It was exciting to observe that the product distributions from EG electro-oxidation in AEM-DEGFC are closely consistent with the results obtained from the electrochemical study in the three-electrode cell with the on-line sample collection system.

2. Experimental

2.1. Preparation of catalysts

The Pt/C and Au/C catalysts were synthesized through a modified solution-phase reduction method recently developed in our group [23–25]. The main synthesis procedures are described below:

2.1.1. Pt/C

$Pt(acac)_2$ (0.5 mmol, Acros Organics), oleylamine (200 μl, Aldrich Chemistry) and oleic acid (200 μl, Fisher Chemistry) were first dissolved in a well-mixed ink of Vulcan XC-72R carbon black (146 mg, Cabot) and benzyl ether (40 ml, Acros Organics, 99%) at 60 °C under a nitrogen flow. 1.0 ml $LiBEt_3H$ (1 M in THF, Sigma Aldrich) was quickly injected into the system as the temperature was increased to 120 °C. After being held for 30 min, the temperature was slowly increased to 180 °C and held for an additional 30 min. The Pt/C catalyst was collected after filtration, washing with copious ethanol, and drying in vacuum oven at 50 °C overnight. The Pt/C has a metal loading of 40 wt%, determined by measuring the weight differences between the carbon support and final Pt/C catalyst.

2.1.2. Au/C

$AuCl_3$ (0.5 mmol, Alfa Aesar) was mixed with octadecene (16 ml, Acros Organics) and oleylamine (4 ml, Aldrich Chemistry) under a nitrogen blanket. The system was then rapidly heated to 80 °C, subsequently followed by a quick injection of 1.5 ml $LiBEt_3H$ (1 M in THF, Sigma–Aldrich). After holding the temperature for 10 min, the solution was cooled down to room temperature and separated by centrifugation. The as-prepared Au-NPs were deposited on Vulcan XC-72R carbon black (148 mg, Cabot) to obtain a Au/C catalyst with a 40 wt% metal loading.

2.2. Characterizations of catalysts

The Au/C and Pt/C catalysts were characterized by a transmission electron microscopy (TEM, JEOL 2010) with an operating voltage of 200 kV. X-ray diffraction (XRD) patterns were collected by a Scintag XDS-2000 θ/θ diffractometer using Cu K_α radiation (λ = 1.5406 Å), with a tube current of 35 mA and a tube voltage of 45 kV.

2.3. Electrocatalytic oxidation of EG in a three-electrode cell with an on-line sample collection system

Electrocatalytic oxidation of EG was conducted in a single compartment three-electrode cell setup, equipped with a glass carbon working electrode, an Hg/HgO (1.0 M KOH) reference electrode and a Pt wire counter electrode. Prior to the experiments, 2.0 mg Au/C or Pt/C catalyst was dispersed in 1.0 ml isopropanol by sonication to form uniform ink. The working electrode was prepared by dropping 40 μl of the catalyst ink on the glassy carbon electrode. 20 μl of 0.05 wt% AS-4 anion conductive ionomer solution was then added on the top to bind the catalyst. To investigate the EG oxidation pathways, staircase linear scans with an increment of 100 mV 10 min^{-1} were used for 1.0 M KOH + 0.5 M EG, 1.0 M KOH + 0.5 M glycolic acid, and 1.5 M KOH + 0.5 M oxalic acid solutions. The instantaneous oxidation products at different potentials were on-line collected through a self-designed needle that was positioned within 0.5 mm of the center of the working electrode surface [24,25]. The needle configurations were cleaned with copious de-ionized water before use. The flow rate of sample collection was controlled by a peristaltic pump (Gilson miniplus 3) at 50 μl min^{-1}. At each potential, 0.5 ml of sample was collected in 10 min and stored in a 2 ml screw cap vial (Agilent) for HPLC analysis. All voltages were reported with respect to standard hydrogen electrode (SHE).

2.4. Electrocatalytic oxidation of EG in anion exchange membrane - direct ethylene glycol fuel cells (AEM-DEGFCs)

The fuel cell tests were performed on a Scribner Fuel Cell System 850e (Scribner Associates, USA). The fuel cell fixture with an active area of 5 cm^2 was purchased from Fuel Cell Technology Inc. The anode end plate was made of stainless steel (316L) so as to tolerate the alkaline environment. The anode catalyst ink was made by mixing water-dispersed 10 wt% of PTFE and Pt/C (or Au/C) powder. The ink was sprayed onto carbon cloth that was used as liquid diffusion layer (LDL). For the cathode, a commercial non-PGM HYPERMECTM catalyst (Fe-Cu-N_4/C, Acta) blended with AS-4 anion conductive ionomer (Tokuyama) was directly sprayed onto the anion exchange membrane (AEM, Tokuyama A201, 28 μm). 25CC carbon paper (SGL Group) was applied as the cathode gas diffusion layer (GDL). The

membrane electrode assembly (MEA) was fabricated by mechanically sandwiching the anode, AEM, and cathode together. 1.0 M or 0.1 M EG in 2.0 M KOH was fed into the anode compartment at 4 ml min^{-1}.High purity O_2 (99.999%) regulated at 400 ml min^{-1} was fed into the cathode compartment under a back pressure of 30 psi. After the MEA was fully activated by fast operating the voltage from the open circuit voltage (OCV) to 0.1 V for 30 cycles, the polarization curves of the AEM-DEGFCs were obtained by scanning current and collecting the respective voltage and power density. The studies of selective electrocatalytic oxidation of EG and glycolic acid were carried out by looping 55 ml of EG or glycolic acid alkaline electrolyte from a plastic fuel vessel into the anode compartment at 50 °C and with the same O_2 flow rate and back pressure at the cathode compartment. The EG oxidation was performed for 2 h for each constant voltage. During the tests, the anode overpotential was monitored by a Hg/HgO (1.0 M KOH) electrode, and reported with respect to SHE. In the meantime, the current density and power density generated were recorded. The temperatures of anode fuel, cathode humidifier, and fuel cell were kept at 50 °C. Samples were collected after the 2-h reaction period for HPLC analysis. It should be mentioned that all the investigated products were in their deprotonated (salt) forms in alkaline media, however, for the convenience of comparison with previous studies, we reported them in their acid forms (except for CO_2) throughout this paper. The selectivity was calculated as follows [16,24–28]:

$$\text{Selectivity} = \frac{\text{Moles of specific product forms}}{\text{Total moles of } C_1 \text{ and } C_2 \text{ products detected}} \times 100\% \quad (1)$$

The carbon balance was based on the following [16,24,25]:

$$\text{Carbon balance} = \frac{2M_{C_i} - 2M_{C_2} - M_{C_1} - 2M_{C_f}}{2M_{C_i}} \times 100\% \quad (2)$$

Assuming that no formic acid was further oxidized to carbonate (CO_2 combined with OH^- in high pH media) then,

$$M_{C_1} = M_{C_{FA}} \quad (3)$$

Therefore:

$$\text{Carbon balance} = \frac{M_{C_i} - M_{C_2} - 1/2M_{C_{FA}} - M_{C_f}}{M_{C_i}} \times 100\% \quad (4)$$

where M_{C_i} and M_{C_f} are the initial and final moles of EG in the electrolyte. M_{C_2}, M_{C_1} and $M_{C_{FA}}$ are the moles of C_2 products (glycolic acid, glyoxylic acid, oxalic acid), C_1 products (formic acid and carbonate), and formic acid (FA) respectively. A smaller carbon balance indicates less formic acid was further oxidized to carbonate.

2.5. Products analysis

The EG oxidation products in three-electrode cell and under different fuel cell operation voltages were analyzed using a high performance liquid chromatography (HPLC, Agilent 1100), equipped with a refractive index detector (RID, Agilent G1362A) and a variable wavelength detector (VWD, Agilent G1314A, 220 nm). An OA-1000 column (Alltech, 60 °C) with an eluent of 5 mM aqueous sulfuric acid (0.3 ml min^{-1}) was applied for the products separation. 20 μl of each sample was injected into the HPLC system. All products were identified by comparison with authentic samples.

3. Results and discussion

3.1. Physical characterizations

The XRD patterns of Pt/C and Au/C catalysts are shown in Fig. 1a, both of which display a typical face-centered cubic (FCC) structure. The average metal crystal sizes of Pt/C and Au/C catalysts calculated based on their (2 2 0) diffraction peaks are 1.9 and 2.7 nm, respectively, using the Debye–Scherrer formula [29,30]. Typical TEM images of Pt/C and Au/C and their corresponding size histograms are shown in Fig. 1b and c. It is observed that most of the nanoparticles are round in shape and uniformly dispersed on the carbon support with few agglomerations. The average particle sizes evaluated from the TEM images are 2.4 and 3.5 nm for Pt/C and Au/C, respectively, which are in good agreement with the results from the XRD analyses. The histograms of particle sizes counted from 100 randomly chosen Pt or Au particles in arbitrary areas show a narrow size distribution of 1–4 nm for Pt/C and 2–6 nm for Au/C. The similar particle size and size distribution of Pt/C and Au/C provide a good platform for investigating selective electro-oxidation of EG in alkaline electrolyte.

3.2. Selective electro-oxidation of EG on Pt/C and Au/C catalysts in three-electrode cell with an on-line sample collection system

Fig. 2 shows the staircase linear scans for electro-oxidation of EG on Pt/C and Au/C in alkaline solution, alongside the products distribution as a function of applied potential. The onset potential of 0.5 M EG oxidation in 1.0 M KOH solution on Pt/C is 0.3 V, which is around 400 mV more negative than that on Au/C (0.7 V). The peak current density obtained on Pt/C (38 mA cm^{-2}) is also higher than that on Au/C (15 mA cm^{-2}). As expected, Pt/C exhibits a higher activity toward EG oxidation compared with Au/C in alkaline media, due to the stronger adsorption of hydroxyl group and better electrocatalytic properties of Pt [9,31]. Whereas, a reasonable catalytic activity toward EG oxidation on Au needs a higher applied potential to achieve a sufficient degree of coverage of adsorbed OH^- to facilitate the H_β abstraction [9,17,31]. It was reported that the OH^- adsorption was enhanced in alkaline media, which initiated at 0.4 V and 0.6 V vs. SHE on Pt and Au, respectively [31,32]. This is in good agreement with the onset potential of oxidation of 0.5 M EG in 1.0 M KOH solution on Pt/C (ca. 0.3 V vs. SHE) and Au/C (ca. 0.7 V vs. SHE), as shown in Fig. 2a and b.

During the staircase linear scans, the instantaneous oxidation products at different potentials were on-line collected through a self-designed needle positioned near the center of Pt/C (Au/C) deposited working electrode, and analyzed by HPLC. Fig. 2a shows that on the Pt/C catalyst, only glycolic acid, oxalic acid and formic acid were detected as the stable products in liquid electrolyte, which can represent the local products distribution near the working electrode surface during the sweep of the applied potentials. The first observed product, glycolic acid, was detected since 0.3 V, which is in agreement with the observed onset potential. This suggests that the on-line sample collection system is able to effectively catch the instant oxidation products generated near the catalyst surfaces. As the potential increases, the concentration of glycolic acid steeply ramps up until 0.9 V, which corresponds to the potential of peak current density in staircase linear voltammetry. It has been demonstrated that at ca. 0.85 V, Pt starts to form surface oxide, which blocks the active sites of Pt [21,22]. Therefore, the concentration of glycolic acid, along with the current density in voltammetry, decreases while the potential is higher than 0.9 V. Oxalic acid and formic acid were also observed as products with relatively low concentrations starting from 0.6 V. The concentration of oxalic acid reaches its peak at 1.0 V, and subsequently decreases at higher applied potentials. Interestingly, the concentration of formic acid first increases slowly until 0.9 V, where the highest current density is obtained, and then its concentration starts to decrease due to the formation of PtO_x. As the applied potential reaches 1.1 V, the concentration of formic acid increases again, and its accelerated increasing from 1.5 V to 1.7 V may count for the slight increase in current density.

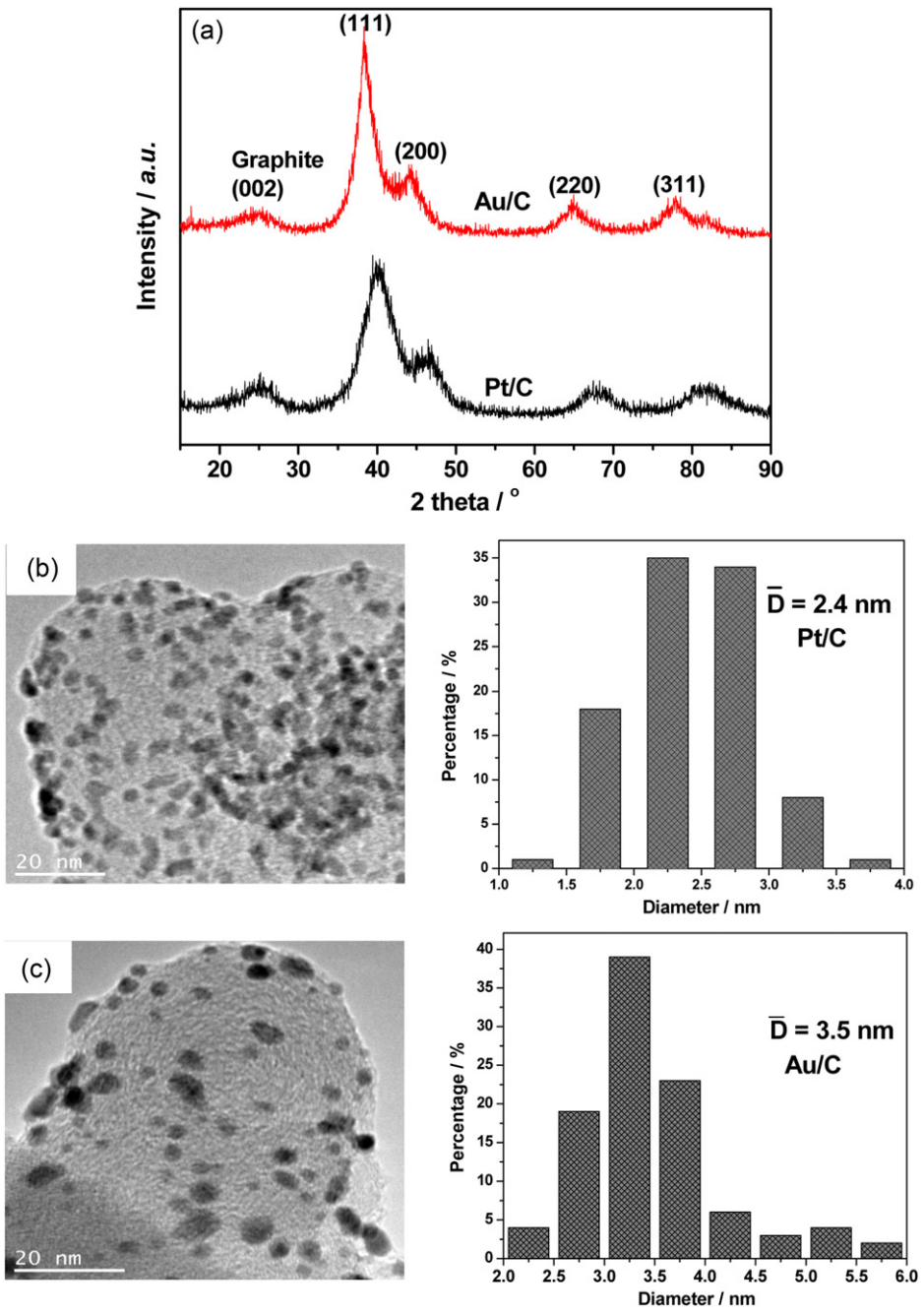

Fig. 1. XRD patterns (a), TEM images and particle size distributions of Pt/C (b) and Au/C (c) catalysts.

Different from Pt/C, only two products – glycolic acid and oxalic acid were detected on Au/C in the potential region investigated. As shown in Fig. 2b, the appearance of the dominant product glycolic acid, commences at 0.7 V and shows its peak concentration at 1.3 V, potential corresponding to the peak current density of EG oxidation. At an applied potential higher than 1.3 V, which has been reported the onset potential of surface Au oxide formation [22,31,33], the concentration of glycolic acid decreases sharply. It implies that AuO_x is nearly inactive to EG oxidation under the experiment conditions performed in this study. The concentration profile of formic acid has a similar trend as that of glycolic acid, except that it begins to be detected as a product at 1.0 V, which is 300 mV more positive than glycolic acid. A significant difference between EG oxidation on Au/C and Pt/C is that oxalic acid is absent from the product distribution profile on Au/C over the whole range of applied potentials.

Based on the results discussed above, it is clear that glycolic acid is an important reaction intermediate in the process of EG oxidation on both Pt/C and Au/C catalysts. In order to gain deep insights to the pathways of electro-oxidation of EG in alkaline solution, glycolic acid was used as a reactant in independent cyclic voltammetry (CV) experiments, which were conducted with a scan rate of 50 mV s^{-1}. The cyclic voltammograms of 0.5 M glycolic acid oxidation on Pt/C and Au/C in 1.0 M KOH are shown in Fig. 3a and b. Compared with the CV curve recorded in only 1.0 M KOH, Pt/C with addition of 0.5 M glycolic acid produced a 3 orders of magnitude higher peak current density. On the contrary, nearly no current was generated from glycolic acid oxidation on Au/C at a potential of less than1.2 V, and only

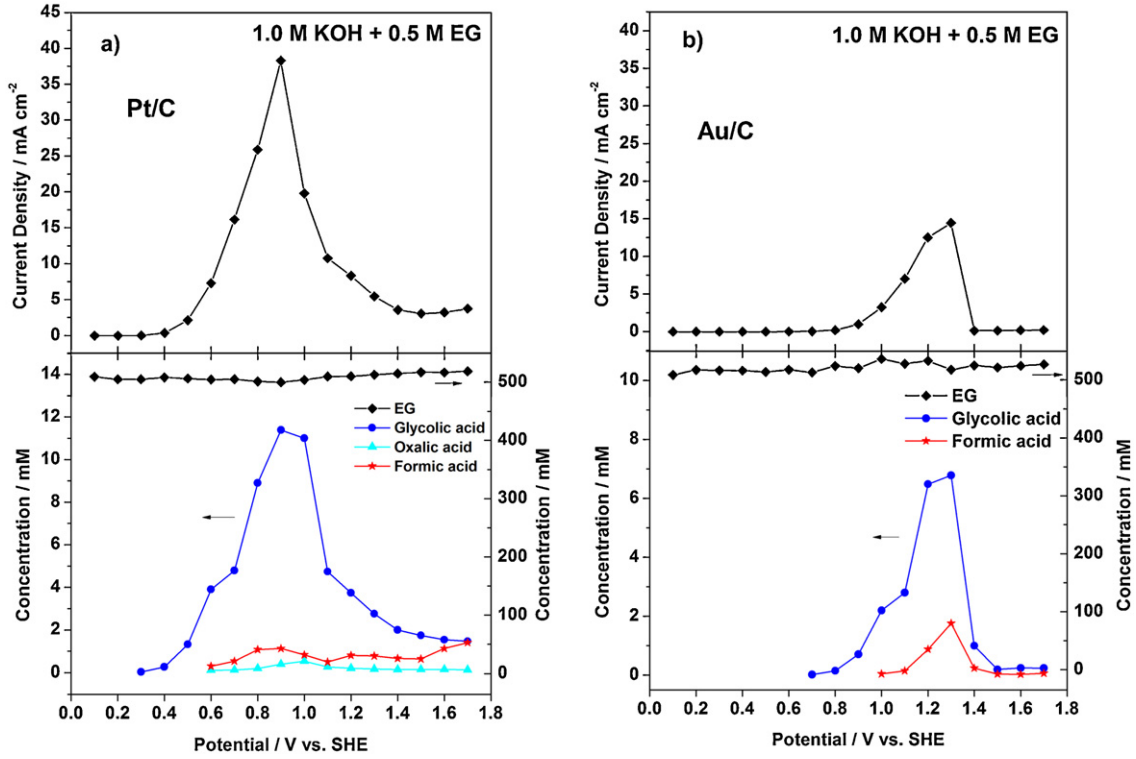

Fig. 2. Polarization curves and product concentrations of electrocatalytic oxidation of EG on Pt/C (a), Au/C (b) in 1.0 M KOH + 0.5 M EG in a three-electrode cell with an on-line sample collection system.

a very small oxidation current was detected on Au/C at a potential of greater than 1.2 V in 1.0 M KOH solution + 0.5 M glycolic acid. This observation agrees well with the results reported by Kadirgan et al. that glycolate is the only product on Au at potential below 1.13 V vs. SHE, whereas at potentials above 1.13 V, glycolate could be further oxidized to glyoxylate, oxalate and formate, based on liquid chromatography (HPLC) and infrared spectroscopy (FTIR) analysis [9,10]. Our recent electrolysis cell study also showed that under a very high ratio of Au/C to glycolic acid (ca.9500 times higher than this experiment) in a carbon cloth-based liquid diffusion layer configuration, glycolic acid can be further oxidized to oxalic acid [25]. It suggests the reactor configuration (such as the metal to fuel ratio) also has a significant effect on the final product distribution. It can also be concluded that Pt/C is much more active than Au/C for the electrocatalytic oxidization of glycolic acid in alkaline media, and the only product is oxalic acid. The cyclic voltammogram of 0.5 M oxalic acid oxidation in 1.5 M KOH on Pt/C was also tested, and compared with that of a blank 1.0 M KOH (Fig. 3c). Their similar CV curves suggest that oxalic acid is a stable reaction product, and Pt is nearly inert to its further oxidation (C—C bond cleave of oxalic acid to carbonate).

The staircase linear scan voltammetry was conducted in 1.0 M KOH solution + 0.5 M glycolic acid on Pt/C. The results shown in Fig. 4 indicate that on Pt/C, the peak current density produced from glycolic acid oxidation (8.5 mA cm^{-2}) is smaller than that produced from 1.0 M KOH + 0.5 M EG solution (38 mA cm^{-2}), although the oxidation of both EG and glycolic acid have the same onset potential of 0.4 V. This indicates that Pt/C has higher activity toward EG oxidation than glycolic acid oxidation. However, their different product distributions may account for the difference in their produced current densities. Compared to the 4-electrons-transfer from glycolic acid oxidation to oxalic acid, oxalic acid and formic acid produced from EG oxidation involve 8- and 6-electrons-transfer, respectively; this will contribute to the higher generated current. The current density of glycolic acid oxidation features two peaks: the bigger one centered at 0.8 V can be attributed to its oxidation on clean Pt surface, while the smaller one centered at 1.1 V is due to the catalytic activity of PtO_x at high potentials (>1.0 V).

Samples were collected during the staircase linear scan and analyzed by HPLC. The major product, oxalic acid starts to appear at 0.3 V and its concentration increases until 0.8 V, beyond which it drops until 1.0 V because of the surface oxide formation. Then, a small peak is shown at 1.1 V, suggesting PtO_x is catalytically active toward glycolic oxidation at a higher potential, after which the concentration of oxalic acid decreases. A very small amount of glyoxylic acid was detected from 0.6 V, which is 300 mV behind the oxalic acid detection. Glyoxylic acid is a reaction intermediate for glycolic acid oxidation to oxalic acid. However, it has been found that the oxidation of aldehyde group proceeds much faster than hydroxyl group [34]. Thus, the glyoxylic acid was not detected until higher potentials are applied (i.e. >0.6 V), at which more glycolic acid was generated and participated into the reaction, and thus glyoxylic acid can be caught by the on-line collection system. Compared with the product distribution of EG oxidation on Pt/C, the absence of formic acid within the whole applied potentials suggests the C_1 product formic acid was not derived from the further oxidation of glycolic acid, but rather derived from direct C—C bond breaking of EG on the Pt surface at relative high potential (e.g. >0.6 V). On the contrary, Au/C is inert to the glycolic acid oxidation, and no products, such as glyoxylic acid, oxalic acid and formic acid, were detected in the entire potential range (0–1.7 V) using HPLC analysis, suggesting that on Au/C, glycolic acid is a fairly stable reaction intermediate for EG oxidation under the investigated experimental conditions.

3.3. Proposed pathways for electro-oxidation of EG on Pt/C and Au/C in alkaline media

Based on the results obtained from our three-electrode cell with the on-line sample collection system, we proposed reaction

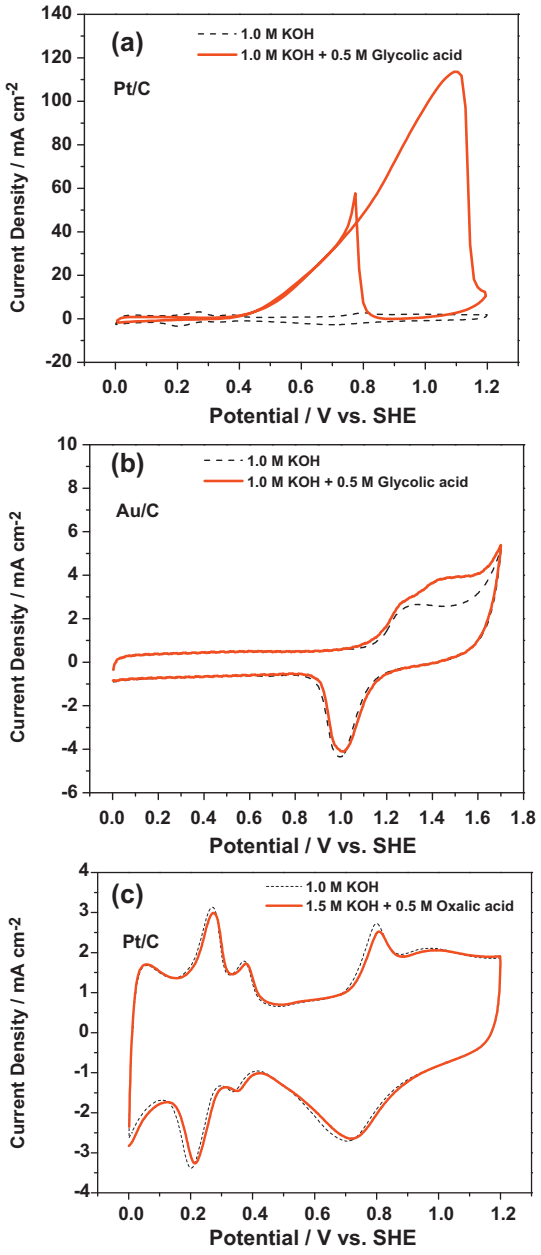

Fig. 3. Cyclic voltammograms of Pt/C (a) and Au/C (b) in 1.0 M KOH + 0.5 M glycolic acid, and Pt/C (c) in 1.5 M + 0.5 M oxalic acid with a scan rate of 50 mV s^{-1}.

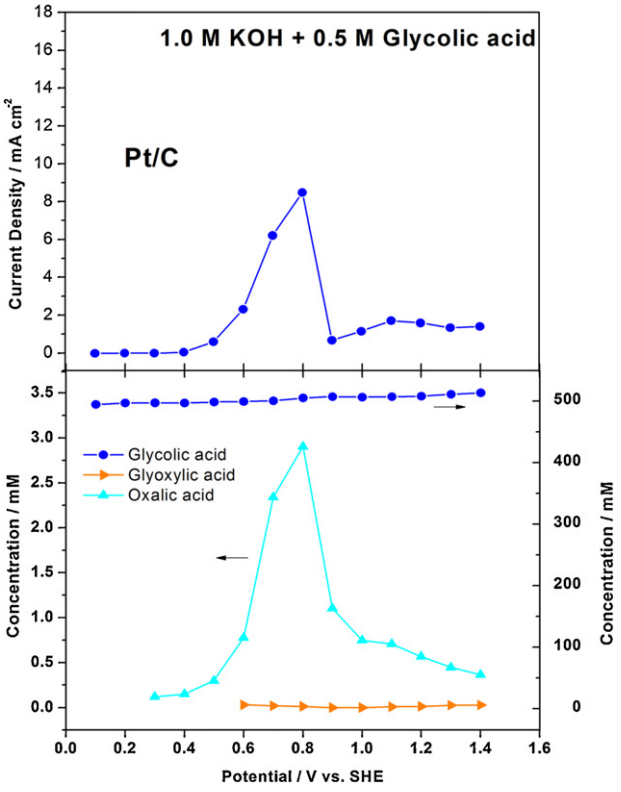

Fig. 4. Polarization curves and product concentrations of electrocatalytic oxidation of glycolic acid on Pt/C in 1.0 M KOH + 0.5 M glycolic acid in a three-electrode cell with an on-line sample collection system.

pathways for EG oxidation on Pt/C and Au/C in alkaline solution, as shown in Fig. 5. It has been reported that glycolaldehyde is the first intermediate formed on Pt via the solution and metal catalyzed steps [16,17]. Previous electrochemical in situ FTIR study also examined the adsorbed glycolaldehyde on Pt electrode during EG electro-oxidation [18]. However, glycolaldehyde is not stable in alkaline solution and will decompose through non-Faradic reaction [17]. In order to clarify the role of glycolaldehyde in EG electro-oxidation, comparison experiments were carried out using 10 mM glycolaldehyde + 1.0 M KOH with and without the applied potentials (0.6 V or 0.9 V vs. SHE) in the absence of oxygen. Samples were taken out after 10 min and immediately neutralized with equal moles of H_2SO_4, this is in agreement with the sample withdraw intervals (10 min for each potential) during the online sample collection process in the three-electrode cell experiments. Various glycolaldehyde decomposition products including formic acid, glyceric acid, erythrose etc. were detected by HPLC, regardless of the potentials applied. It is interesting to find that the concentration of formic acid generated in 10 min with and without the applied potential (0.6 V or 0.9 V vs. SHE) were nearly the same: no potential applied: 2.3 mM, 0.6 V: 2.3 mM, and 0.9 V: 2.4 mM. It suggests that in alkaline media formic acid was not favorably produced by further electro-oxidizing glycolaldehyde on Pt/C catalyst, but merely a glycolaldehyde decomposition product. Furthermore, it was shown in Fig. 2a that in the whole studied potential ranges (0.3–1.7 V vs. SHE) during the electro-oxidation of EG on Pt/C in alkaline solution, other glycolaldehyde decomposition products (such as glyceric acid, erythrose etc.) were not observed in liquid electrolyte by the HPLC analysis. Therefore, the absence of these products from the non-Faradic reaction of glycolaldehyde strongly indicates that the dominant reaction intermediate (glycolaldehyde) formed on the surface of Pt/C was readily further oxidized to glycolic acid, starting at 0.3 V, without any noticeable desorption to form "glycolaldehyde in solution-phase", therefore its decomposition reaction would not occur.

Subsequently, two reaction pathways proceed in parallel for electro-oxidation of EG at potentials >0.6 V: 1) the hydroxyl group of glycolic acid is oxidized to produce glyoxylic acid, which is rapidly oxidized to oxalic acid; 2) EG directly dissociates its C—C bond to form formic acid, which possibly generates adsorbed CO species, and finally carbonate, according to previous in situ FTIR spectroscopic [9,11,18,19] and DEMS [35] studies. Interestingly, PtO_x also shows activity to promote the EG oxidation to oxalic acid through stepwise oxidation of EG without C—C breaking, and to formic acid through the direct dissociation of EG at higher potential range of >1.0 V. Neither Pt nor PtO_x demonstrates activity to the oxidation of oxalic acid (Fig. 3c). On Au/C, the oxidation of EG occurs at 0.7 V, which is 400 mV more positive than that on Pt/C. Similar to Pt/C, the glycolaldehyde decomposition products on Au/C were absent from the product profile. The higher onset potential of

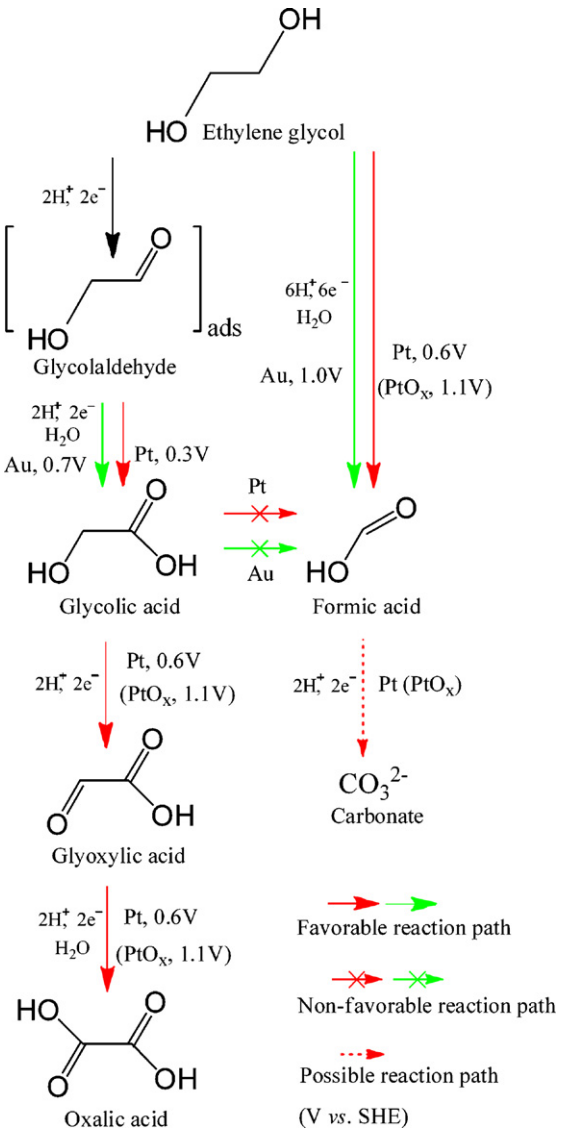

Fig. 5. The proposed pathways for electrocatalytic oxidation of EG on Au/C and Pt/C in alkaline media, the starting potentials for observed reaction paths are marked.

EG oxidation on Au/C possibly makes the glycolaldehyde a quite reactive intermediate, which is quickly oxidized to glycolic acid, thus, cannot be detected in solution. This is similar to glycerol electro-oxidation: no glyceraldehyde but only glyceric acid was detected from glycerol oxidation [22]. Its first product, glycolic acid, is very difficult to be further oxidized. As the applied potential is higher than 1.0 V, where OH_{ads} starts to accumulate on the Au surface, the C—C bond of EG is directly broken to yield formic acid.

Extensive studies have been conducted to investigate their EG oxidation pathways on Pt and Au electrodes [10,12–14,36,37], however, detailed reaction paths still need to be clarified. It has been generally accepted that two reaction pathways proceed on Pt/C: a poisoning path that involves C—C breaking of C_2 chemicals to produce CO, and a non-poisoning path that stops at oxalic acid. Our results confirmed that oxalic acid is a fairly stable oxidation product that hurdles further C—C scission to C_1 products on Pt/C. Furthermore, we found that the C—C bond cleavage is not a favorable process on other C_2 reaction intermediates, such as glycolic acid and glyoxalic acid, while the successive oxidation of hydroxyl (—OH) or carbonyl (C=O) to deeper-oxidized chemicals is a dominant process. We clarified that the C—C bond cleavage mainly occurs on EG both for Pt/C and Au/C. This may be due to its symmetric structure

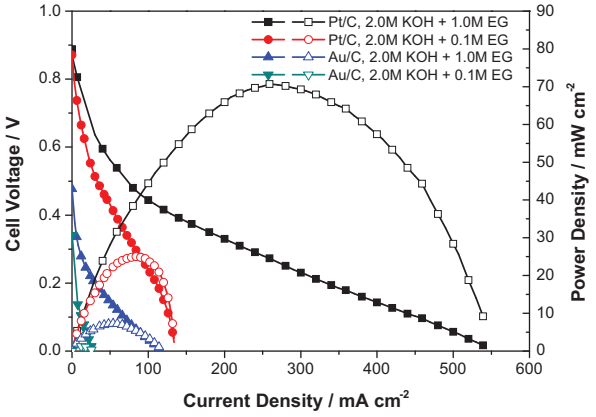

Fig. 6. Polarization and power density curves of AEM-DEGFC at 50 °C. Anode: Pt/C or Au/C (40 wt%), 1.0 mg_{metal}/cm^{-2}, cathode: Fe-Cu-N_4/C (Acta 4020), 1.0 mg_{cat}/cm^{-2}. Membrane: Tokuyama A201, 28 μm, 2.0 M KOH + 1.0 M EG or 2.0 M KOH + 0.1 M EG, O_2: 0.4 L min^{-1}, 30 psi.

and a favorable O bridge adsorption on the catalyst surface [38]. Predominant cleavage of the C—C linkage of EG to yield solely formate has been observed on NiO film in 0.5 M KOH at very high potential (i.e. >1.4 V vs. SHE) using electrochemical FTIR [18]. Recently, Koper's group found that dissociation of C—C bond of glyceric acid to form glycolic acid on both Au and Pt electrodes in relatively high potentials. This also occurs on the C—C containing two adjacent —OH groups [22]. Combining our new observations, we hypothesize that C—C bond cleavage is a common process that occurs on vicinal diol compounds, such as EG and glyceric acid, on both Pt and Au catalysts in relatively high potentials (i.e. 0.6 V for Pt and 1.0 V for Au).

3.4. Electro-oxidation of EG in AEM-DEGFC with Pt/C and Au/C anode catalysts

In order to examine the proposed reaction pathway, we used single AEM-DEGFC to further investigate electrocatalytic oxidation of EG. In an AEM-DEGFC, Pt/C or Au/C with a loading of 1.0 mg cm^{-2} was employed as the anode catalyst, while a commercial non-PGM HYPERMECTM (Fe-Cu-N_4/C, Acta, 1.0 mg cm^{-2}), which is inert to alcohol oxidation, was used as the cathode catalyst. The anode overpotential was on-line monitored by an Hg/HgO (1.0 M KOH) reference electrode. The polarization and power density curves are shown in Fig. 6. Compared with Pt/C, the fuel cell performance is much lower when using Au/C anode catalyst. In particular, when fed with 2.0 M KOH + 1.0 M EG into the anode compartment, the AEM-DEGFC with the Pt/C anode catalyst yields an open circuit voltage (OCV) of 0.868 V and a peak power density of 71.0 mW cm^{-2} at 259 mA cm^{-2} at 50 °C, while for the AEM-DEGFC with the Au/C anode catalyst, an OCV of 0.478 V and a peak power density of 7.3 mW cm^{-2} at the current density of 60 mA cm^{-2} were achieved. Around 400 mV greater OCV obtained on Pt/C than on Au/C closely agrees with the 400 mV more negative onset potential observed on Pt/C compared with Au/C in the three-electrode cell setup, where the same concentration ratio of KOH to EG (2:1) was used. In addition, the higher fuel cell peak power density obtained on Pt/C as compared with Au/C is also consistent with higher generated current density from EG oxidation on Pt/C observed in the staircase linear scan voltammetry. It is observed that the fuel cell voltage dropped more rapidly when the EG concentration was switched from 1.0 M to 0.1 M, in a fixed 2.0 M KOH electrolyte, giving rise to the decreased power density of 25 mW cm^{-2} and 1.3 mW cm^{-2} on Pt/C and Au/C, respectively. Furthermore, the limiting current density also decreased from 539 mA cm^{-2} to 134 mA cm^{-2} on Pt/C, and

Table 1
Electrocatalytic oxidation of EG on Pt/C in AEM-DEGFC with 2.0 M KOH + 1.0 M or 0.1 M EG at different fuel cell operation voltages for 2 h, 50 °C.

Pt/C	Cell voltage (V)	Anode overpotential (V vs. SHE)	Selectivity (%)				EG conversion (%)	Current density (mA cm^{-2})	Power density (mW cm^{-2})	Carbon balance (%)
			C_2 acids	Glycolic acid	Oxalic acid	Formic acid				
2.0 M KOH + 1.0 M EG	0.5	0.388	96.3	95.0	1.3	3.7	10.6	42.7	21.4	3.4
	0.3	0.439	96.4	93.5	2.9	3.6	31.6	177.1	53.0	5.5
	0.1	0.493	95.3	83.0	12.3	4.7	51.7	332.1	33.2	8.8
2.0 M KOH + 0.1 M EG	0.5	0.432	94.7	92.7	2.0	5.3	39.3	23.3	11.7	3.2
	0.3	0.541	91.8	80.2	11.6	8.2	94.9	80.2	24.0	16.5
	0.1	0.712	91.3	62.2	29.1	8.7	99.7	100	10.0	25.0

114 mA cm^{-2} to 26 mA cm^{-2} on Au/C. This can be explained by the fact that the diluted EG cannot provide sufficient reactant to the catalyst active sites, especially in the high current density region, where a high mass transfer rate is needed.

The product distribution and electricity generation from electrocatalytic oxidation of EG was investigated in real AEM-DEGFC with Pt/C or Au/C anode catalyst. 55 ml of 2.0 M KOH + 1.0 M EG was looped from a plastic fuel vessel into the anode compartment at 50 °C for 2 h, meanwhile, high purity O_2 with a flow rate of 0.4 l min^{-1} was pumped into the cathode compartment under a back pressure of 30 psi. The EG oxidation was performed by applying different constant fuel cell voltages, while the anode overpotential was monitored in situ and reported with respect to SHE. The oxidation products were analyzed by HPLC after each 2-h operation. As the fuel cell operation voltage was controlled at 0.5 V, 0.3 V and 0.1 V, the average power density and current density of an AEM-DEGFC with the Pt/C within 2-h reaction were 21.4 mW cm^{-2} at 42.7 mA cm^{-2}, 53.0 mW cm^{-2} at 177.1 mA cm^{-2}, and 33.2 mW cm^{-2} at 332.1 mA cm^{-2}, respectively, as shown in Fig. 7a and summarized in Table 1. These current density and power density are slightly lower than the values observed in regular *I–V* scan with open circuit of fuel. This is due to the gradual decrease of EG concentration during the 2 h reaction with closed circuit of fuel. In addition, the on-line monitored anode overpotential is 0.388 V, 0.439 V and 0.493 V (vs. SHE) on Pt/C at the fuel cell operation voltage of 0.5 V, 0.3 V and 0.1 V, respectively, when the AEM-DEGFC reactor is fed with 2.0 M KOH + 1.0 M EG. Fig. 7a and Table 1 also summarize the oxidation products from EG oxidation in basic environment on Pt/C under different operation voltages. Glycolic acid was observed as the major product, with a selectivity of 83.0–95.0% in the whole fuel cell operation voltage range. Meanwhile, oxalic acid and formic acid also appeared in the final products profiles. This observation is consistent with the product distributions examined from the three-electrode cell system, where all glycolic acid, oxalic acid and formic acid were found at relatively low applied potentials (<0.6 V). Furthermore, it is interesting to note that the fuel cell operation voltage (anode overpotential) is able to tune the product distributions. With the fuel cell voltage decreasing, the selectivity to glycolic acid drops from 95.0% at 0.5 V to 83.0% at 0.1 V. Conversely, the selectivity to oxalic acid and formic acid increase from 1.3% to 12.3%, and 3.7% to 4.7%, respectively. The carbon balance for the AEM-DEGFC operated at 0.5 V, 0.3 V, and 0.1 V are 3.4%, 5.5%. 8.8%, respectively. The high carbon balance at low fuel cell operation voltages indicates that formic acid may be further oxidized to CO, or carbonate on the active Pt/C catalyst. These products escaped the identification of HPLC, but have been probed as the reaction intermediates/products by using the FTIR spectroscopy [9,12,18,39].

In order to elucidate the reaction pathway of intermediate glycolic acid in EG oxidation on Pt/C in AEMFC, 2.0 M KOH + 1.0 M glycolic acid was applied as fuel. It seems that on Pt/C more energy is needed to oxidize glycolic acid than EG, which is evidenced by the higher anode overpotential (0.550–0.661 V vs. SHE) and lower peak power density (24.2 mW cm^{-2}), as observed in Fig. 7b and Table 2. It is also shown that oxalic acid with a selectivity of >98% was obtained, along with production of a small amount of glyoxylic acid (<2% selectivity). In our study, 100% selectivity to C_2 products was achieved without detection of any formic acid even at the fuel cell voltage of 0.1 V, at which the anode overpotential is as high as 0.661 V and the conversion of glycolic acid reaches 38.7%. The appearance of glyoxylic acid is due to the partial oxidation of

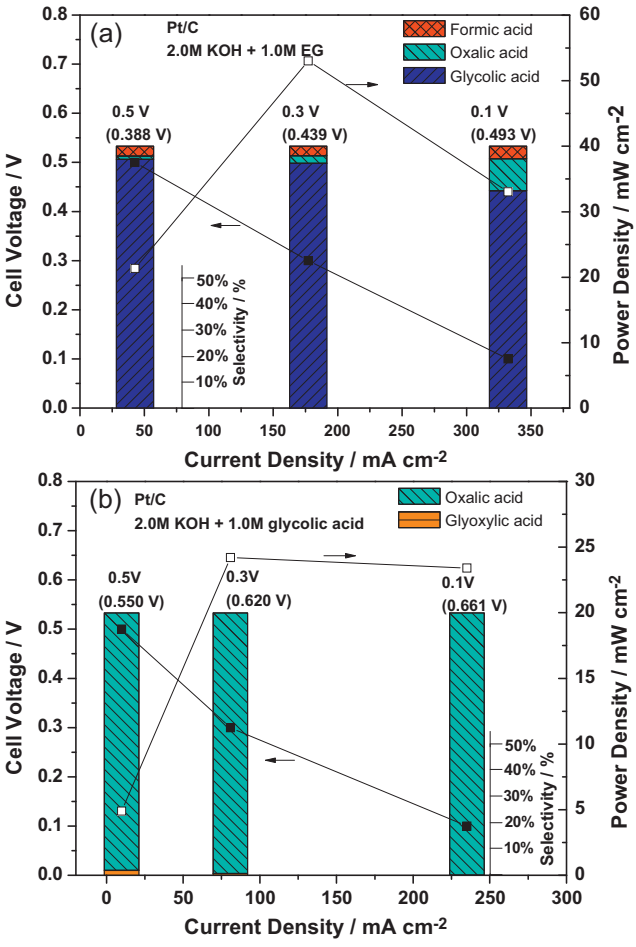

Fig. 7. Product selectivity and electricity generation from electrocatalytic oxidation of EG or glycolic acid on Pt/C with 2.0 M KOH + 1.0 M EG (a) or 2.0 M KOH + 1.0 M glycolic acid (b) in single AEMFC reactor for an operation duration of 2 h at 50 °C. Anode overpotential (vs. SHE) marked in parentheses.

Table 2
Electrocatalytic oxidation of glycolic acid on Pt/C in AEM-DEGFC with 2.0 M KOH + 1.0 M glycolic acid at different fuel cell operation voltages for 2 h, 50 °C.

Pt/C	Cell voltage (V)	Anode overpotential (V vs. SHE)	Selectivity (%)				Glycolic acid conversion (%)	Current density (mA cm^{-2})	Power density (mW cm^{-2})	Carbon balance (%)
			C_2 acids	Glyoxylic acid	Oxalic acid	Formic acid				
2.0 M KOH + 1.0 M glycolic acid	0.5	0.550	100	2.0	98.0	0	0.4	9.9	4.9	4.0
	0.3	0.620	100	0.8	99.2	0	15.3	80.8	24.2	4.1
	0.1	0.661	100	0.2	99.8	0	38.7	235.1	23.4	4.5

glycolic acid, and its selectivity decreasing from 2.0% to 0.2% with the fuel cell potential decreasing from 0.5 V to 0.1 V is because of its further fast oxidation to oxalic acid. Moreover, the carbon balance calculated generally closes to less than 5%, which is within the system error expected in HPLC analysis. Based on the observed results, it is suggested that in AEMFCs, glycolic acid oxidation does not produce formic acid, but produces oxalic acid, which exactly matches the proposed pathways of EG oxidation on Pt/C catalyst in three-electrode cell (Fig. 2a and 4). The C—C bond cleavage occurs directly from EG (not glycolic acid) on Pt/C under fuel cell operations.

In sharp contrast to Pt/C, Au/C is much less active to the EG electro-oxidation in the AEM-DEGMFC with 2.0 M KOH + 1.0 M EG fuel under the working conditions, as evidenced by its lower peak power density (4.8 mW cm^{-2} at 47.9 mA cm^{-2}) and lower EG conversion (3.6% at 0.3 V, and 10.4% at 0.1 V). The on-line monitored anode overpotentials are 0.601 V and 0.694 V for the fuel cell voltage operated at 0.3 V and 0.1 V, respectively, which are obviously higher than that observed on Pt/C, as shown in Fig. 8 and Table 3. However, it is found that on Au/C, EG is oxidized to glycolic acid with nearly 100% selectivity, and no oxalic acid has been detected in the final products. The overall carbon balance for the EG oxidation is far less than 5%, which clearly indicates Au is inactive to further oxidation of formic acid. In addition, 2.0 M KOH + 1.0 M glycolic acid was also used as the anode fuel, but no electricity was generated, confirming that the collected formic acid from EG oxidation does not come from the C—C bond dissociation of glycolic acid but from direct C—C bond breaking of EG under fuel cell operations. Therefore, the results further confirm the pathways of EG oxidation on Au/C proposed in light of EG oxidation pathway in the three-electrode cell with the on-line sample collection system: On Au/C catalyst, the stepwise oxidation of EG without breaking the C—C bond stops at the formation of glycolic acid, and the yield of formic acid results from direct C—C bond scission of EG itself at relatively high anode overpotentials in fuel cells.

When EG concentration decreases from 1.0 M to 0.1 M, it is observed that the current density and power density significantly decreased on both Pt/C and Au/C, together with the anode overpotential shifts more positively, as shown in Fig. 9 and Tables 1 and 3 This suggests that the EG oxidation is related to the ratio of – RO_{ads} and OH_{ads} coverage on the catalyst surface. It is also noted that the EG conversion is strongly affected by its concentration in the feeding fuel. The EG conversion in 2.0 M KOH + 0.1 M EG is much higher than that obtained in 2.0 M KOH + 1.0 M EG. In particular, on Pt/C, the EG conversion at fuel cell operation voltages of 0.5, 0.3 and 0.1 V increases from 10.6%, 31.6% and 51.7% with 1.0 M EG to 39.3%, 94.9% and 99.7% with 0.1 M EG, and on Au/C, the EG conversion at fuel cell operation voltage of 0.1 V increases from 10.4% to 20.9%. Meanwhile, decreasing EG concentration also leads to a

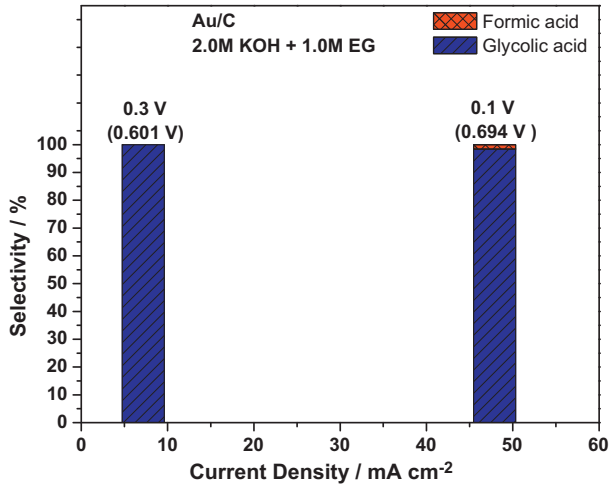

Fig. 8. Product selectivity and electricity generation from electrocatalytic oxidation of EG on Au/C with 2.0 M KOH + 1.0 M EG in single AEM-DEGFC reactor for an operation duration of 2 h at 50 °C. Anode overpotential (vs. SHE) marked in parentheses.

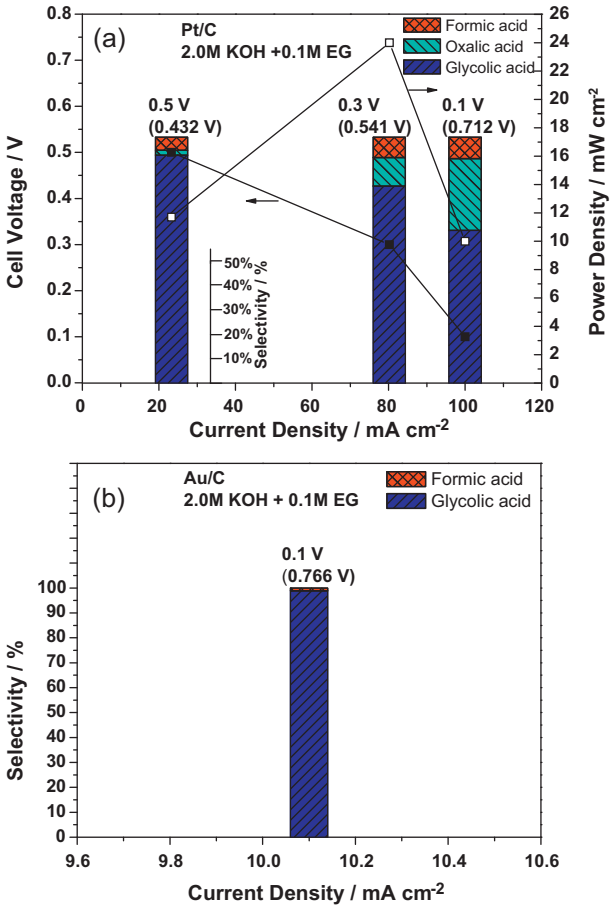

Fig. 9. Product selectivity and electricity generation from electrocatalytic oxidation of EG on Pt/C (a) and Au/C (b) with 2.0 M KOH + 0.1 M EG in single AEM-DEGFC reactor for an operation duration of 2 h at 50 °C. Anode overpotential (vs. SHE) marked in parentheses.

Table 3
Electrocatalytic oxidation of EG on Au/C in AEM-DEGFC with 2.0 M KOH + 1.0 M or 0.1 M EG at different fuel cell operation voltages for 2 h, 50 °C.

Au/C	Cell voltage (V)	Anode overpotential (V vs. SHE)	Selectivity (%)				EG conversion (%)	Current density (mA cm^{-2})	Power density (mW cm^{-2})	Carbon balance (%)
			C_2 acids	Glycolic acid	Oxalic acid	Formic acid				
2.0 M KOH + 1.0 M EG	0.3	0.601	100	100	0	0	3.6	7.2	2.2	0.5
	0.1	0.695	98.4	98.4	0	1.6	10.4	47.9	4.8	0.6
2.0 M KOH + 0.1 M EG	0.1	0.766	99.0	99.0	0	1.0	20.9	10.1	1.0	1.7

lower selectivity of C_2 acids on Pt/C, which further confirms that high applied potential facilitates C—C bond breaking of EG. Still, no oxalic acid was observed from EG oxidation on Au/C anode catalyst in AEM-DEGFC, which suggests that the EG concentration does not apparently change the reaction pathways. The EG oxidation pathways proposed according to the study combining the three-electrode electrolysis cell, on-line sample collection, and HPLC analysis has been well verified by single AEM-DEGFC reactor investigations. This approach is able to not only supplement the previous spectroscopic findings, but also potentially produce new findings on the pathways of electro-oxidation of biorenewable polyols (i.e. glycerol and sorbitol, etc.) on nanostructured metallic catalysts.

4. Conclusions

A modified solution-phase reduction method was used to prepare Pt/C (2.4 nm) and Au/C (3.5 nm), which served as working catalysts for investigation of electrocatalytic oxidation of EG in alkaline media. Our three-electrode cell with on-line sample collection system showed that glycolic acid, oxalic acid and formic acid were sequentially produced from EG oxidation on Pt/C with increasing linear staircase scan voltammetry, while only glycolic acid and formic acid were examined on Au/C. We clarified that formic acid was produced favorably from direct C—C bond cleavage of EG on both Pt/C and Au/C. Further oxidation of glycolic acid to oxalic acid occurs only on Pt/C but not on Au/C at specified test conditions. Electrocatalytic oxidation of EG in single AEM-DEGFCs with Pt/C and Au/C anode catalysts showed consistent results with the three-electrode cell tests. The AEM-DEGFC with Pt/C anode demonstrated a peak power density of 71.0 mW cm^{-2}, which is much higher than that with Au/C anode (only 7.3 mW cm^{-2}) at 50 °C, this is consistent with more negative onset potential and higher generated current density for electro-oxidation of EG on Pt/C than on Au/C obtained in the three-electrode cell setup. With fuel cell operation voltage decreasing (anode overpotential increasing), deeper-oxidized products oxalic acid and formic acid were generated in the Pt/C anode AEM-DEGFC with increased selectivity, and no formic acid was examined when glycolic acid was employed as fuel. On Au/C anode catalyst, very high selectivity of >98% to glycolic acid was achieved. The AEM-DEGFC results confirmed the EG electro-oxidation pathways proposed by using the on-line sample collection system, which is anticipated to be used to explore the reaction sequences for electro-oxidation of other polyols.

Acknowledgments

We acknowledge the US National Science Foundation (CBET-1032547) for funding. Acknowledgment is also made to the donors of the American Chemical Society Petroleum Research Fund and the REF-RS fund of Michigan Tech for partial support of this research. We thank Profs. Susan Bagley and David Shonnard for their help with our HPLC analysis and fruitful discussion. Ji Qi is grateful to the financial support from Chinese Scholarship Council.

References

[1] R. Parsons, T. Vandernoot, Journal of Electroanalytical Chemistry 257 (1988) 9–45.
[2] S. Wasmus, A. Kuver, Journal of Electroanalytical Chemistry 461 (1999) 14–31.
[3] C. Lamy, C. Coutanceau, J.M. leger, Catalysis for Sustainable Energy Production, Wiley-VCH Verlag GmbH & Co. KGaA, 2009, pp. 281-304.
[4] E. Antolini, E.R. Gonzalez, Journal of Power Sources 195 (2010) 3431–3450.
[5] A. Serov, C. Kwak, Applied Catalysis B 97 (2010) 1–12.
[6] E.H. Yu, U. Krewer, K. Scott, Energies 3 (2010) 1499–1528.
[7] N. Ji, T. Zhang, M.Y. Zheng, A.Q. Wang, H. Wang, X.D. Wang, J.G.G. Chen, Angewandte Chemie International Edition 47 (2008) 8510–8513.
[8] M.-Y. Zheng, A.-Q. Wang, N. Ji, J.-F. Pang, X.-D. Wang, T. Zhang, ChemSusChem 3 (2010) 63–66.
[9] M. Beltowska-Brzezinska, T. Luczak, R. Holze, Journal of Applied Electrochemistry 27 (1997) 999–1011.
[10] F. Kadirgan, E. Bouhiercharbonnier, C. Lamy, J.M. Leger, B. Beden, Journal of Electroanalytical Chemistry 286 (1990) 41–61.
[11] P.A. Christensen, A. Hamnett, Journal of Electroanalytical Chemistry 260 (1989) 347–359.
[12] W. Hauffe, J. Heitbaum, Electrochimica Acta 23 (1978) 299–304.
[13] W. Hauffe, J. Heitbaum, Physical Chemistry Chemical Physics 82 (1978) 487–491.
[14] K. Matsuoka, Y. Iriyama, T. Abe, M. Matsuoka, Z. Ogumi, Electrochimica Acta 51 (2005) 1085–1090.
[15] K. Matsuoka, M. Inaba, Y. Iriyama, T. Abe, Z. Ogumi, M. Matsuoka, Fuel Cells 2 (2002) 35–39.
[16] B.N. Zope, D.D. Hibbitts, M. Neurock, R.J. Davis, Science 330 (2010) 74–78.
[17] Y. Kwon, S.C.S. Lai, P. Rodriguez, M.T.M. Koper, Journal of the American Chemical Society 133 (2011) 6914–6917.
[18] S.C. Chang, Y.H. Ho, M.J. Weaver, Journal of the American Chemical Society 113 (1991) 9506–9513.
[19] L. Demarconnay, S. Brimaud, C. Coutanceau, J.M. Leger, Journal of Electroanalytical Chemistry 601 (2007) 169–180.
[20] H. Wang, Z. Jusys, R.J. Behm, Journal of Electroanalytical Chemistry 595 (2006) 23–36.
[21] Y. Kwon, M.T.M. Koper, Analytical Chemistry 82 (2010) 5420–5424.
[22] Y. Kwon, K.J.P. Schouten, M.T.M. Koper, ChemCatChem 3 (2011) 1176–1185.
[23] Z. Zhang, K.L. More, K. Sun, Z. Wu, W. Li, Chemistry of Materials 23 (2011) 1570–1577.
[24] Z. Zhang, L. Xin, W. Li, Applied Catalysis B 119–120 (2012) 40–48.
[25] L. Xin, Z. Zhang, Z. Wang, W. Li, ChemCatChem (2012), cctc.201200017.
[26] B.N. Zope, R.J. Davis, Topics in Catalysis 52 (2009) 269–277.
[27] W.C. Ketchie, M. Murayama, R.J. Davis, Topics in Catalysis 44 (2007) 307–317.
[28] S. Carrettin, P. McMorn, P. Johnston, K. Griffin, G.J. Hutchings, Chemical Communications (2000) 696–697.
[29] Z. Zhang, M. Li, Z. Wu, W. Li, Nanotechnology 22 (2011) 015602.
[30] W.Z. Li, C.H. Liang, W.J. Zhou, J.S. Qiu, Z.H. Zhou, G.Q. Sun, Q. Xin, Journal of Physical Chemistry 107B (2003) 6292–6299.
[31] M. Simoes, S. Baranton, C. Coutanceau, Applied Catalysis B 93 (2010) 354–362.
[32] A.C. Chen, J. Lipkowski, Journal of Physical Chemistry B 103 (1999) 682–691.
[33] L.D. Burke, J.M. Moran, P.F. Nugent, Journal of Solid State Electrochemistry 7 (2003) 529–538.
[34] V. Bambagioni, M. Bevilacqua, C. Bianchini, J. Filippi, A. Marchionni, F. Vizza, L.Q. Wang, P.K. Shen, Fuel Cells 10 (2010) 582–590.
[35] D. Bayer, S. Berenger, M. Joos, C. Cremers, J. Tubke, International Journal of Hydrogen Energy 35 (2010) 12660–12667.
[36] C. Lamy, E.M. Belgsir, J.M. Leger, Journal of Applied Electrochemistry 31 (2001) 799–809.
[37] K. Miyazaki, T. Matsumiya, T. Abe, H. Kurata, T. Fukutsuka, K. Kojima, Z. Ogumi, Electrochimica Acta 56 (2011) 7610–7614.
[38] L. Roquet, E.M. Belgsir, J.M. Leger, C. Lamy, Electrochimica Acta 39 (1994) 2387–2394.
[39] F. Kadirgan, B. Beden, C. Lamy, Journal of Electroanalytical Chemistry 143 (1983) 135–152.